SPE 168688 / URTeC 1565038

Horizontal Hydraulic Fracture Design for Optimal Well Productivity in Anisotropic Reservoirs with Different Aspect Ratios

Francisco D. Tovar*, Kyung Jae Lee, Sergio E. Gonzales, Yun Suk Hwang, Andres M. Del Busto, Aderonke A. Aderibigbe, Texas A&M University; Michael J. Economides, University of Houston; and Christine Ehlig-Economides, Texas A&M University

This paper was prepared for presentation at the Unconventional Resources Technology Conference held in Denver, Colorado, USA, 12-14 August 2013.

Summary

The economic feasibility of the exploitation of unconventional resources is highly dependent on the ability of the operator to maximize individual well productivity, making hydraulic fracture design and implementation the defining factor for a successful field development in most cases. Some unconventional reservoirs, as shallow coal bed methane and over-pressured oil and gas shale formations, commonly present the minimum principal stress in the vertical direction, resulting in the occurrence of horizontal hydraulic fractures. Models for the transient flow and pressure behavior of horizontal fractures emanating from vertical wells exist and clearly show distinct performance from those for vertical fractures. This suggests that the widely accepted unified fracture design (UFD) approach to maximize well productivity for vertical and horizontal wells with vertical hydraulic fractures cannot be used for horizontal fractures. Thereafter, the necessity for guidelines to model and design horizontal fractures becomes evident.

This investigation begins by presenting a new set of equations for horizontal fracture design based on the UFD approach, which allows the direct calculation of fracture width, half-length and conductivity for a given proppant number. Later, a reservoir numerical simulator is used to model well productivity behavior for horizontal fractures in homogeneous formations, with or without vertical to horizontal permeability anisotropy and for different aspect ratios as a function of suitably-defined proppant number, dimensionless fracture conductivity, and fracture penetration index parameters.

The findings of this work reveal a complex behavior for horizontal fractures that prohibits the extrapolation of previous generalizations between proppant number, penetration index and dimensionless fracture conductivity established for vertical fractures. For a number of scenarios, new relationships among these variables are provided to guide horizontal fracture design. Anisotropy and reservoir aspect ratio were also found to significantly impact fracture performance. Additionally, a set of multi-variable functions that permit the estimation of maximum achievable productivity index for the horizontal fracture has been fitted, based on commonly known reservoir parameters and the proppant number. This investigation provides a comprehensive framework to assist the design of optimal horizontal fracture geometry that maximizes productivity for a given mass of proppant.

Introduction

The most important objective of a hydraulic fracture treatment is to optimize the well productivity. In the unified fracture design (UFD) methodology, Valkó and Economides (1998), introduced the proppant number, defined as two times the ratio of the propped volume to the reservoir volume, weighted by the proppant-to-matrix permeability ratio. The authors realized that in order to formulate a meaningful technical optimization problem it is necessary to understand that penetration and dimensionless fracture conductivity compete for, and are interrelated by, the propped volume. The study related the dimensionless productivity index under pseudo-steady state (PSS) production as a function of the proppant number and the dimensionless fracture conductivity as defined by Cinco-Ley and Samaniego-V. (1981) as the ratio of the fracture conductivity to the product of formation permeability and fracture half-length. For each proppant number, there is a maximum productivity index (J_{Dmax}) corresponding to an optimum dimensionless fracture conductivity. For proppant number less than 0.1 the optimum fracture conductivity is about 1.6.

The UFD methodology has been widely accepted and applied within the oil and gas industry. More recent studies have addressed some issues in order to extend its applicability for different models and considerations such as non-Darcy flow (Lopez-Hernandez et al. 2004), and single phase and gas condensate flow systems for both PSS and steady state (SS) conditions (Jamiolahmady et al. 2009).

Daal and Economides (2006) considered hydraulically fractured wells in reservoirs with different aspect ratios (y_e/x_e) to calculate the correspondent PSS productivity index. It was found that for small proppant numbers ($N_p < 0.1$) the correlations developed by Valkó and Economides (1998) are still suitable by the application of a simple relationship to acknowledge the new fracture geometry. For larger proppant numbers the authors developed new factors F_{opt}, which account for the departure from the square drainage, and that enable calculation of J_{Dmax} for a large range of aspect ratios and fracture penetration indices.

The study and design of horizontal fractures has become of interest for shallow and over-pressured coal bed methane formations and for highly over-pressured shale formations. A recent case study performed by Larsen (2011) considered the restricted validity of the traditional type curves of uniform-flux fractures when used in formations of limited thickness with large fracturing treatments, because of the significant boundary effects from the top and bottom of the formation. The authors derived and used analytical solutions to model and analyze data from horizontal fractures with both incompressible and compressible flow that can be extended to multilayered models.

This study uses a numerical simulator to investigate relationships between proppant number, dimensionless fracture conductivity and productivity index for horizontal hydraulic fractures, and provides design equations for the productivity optimized design of horizontal fractures considering the impacts of both reservoir aspect ratio and vertical to horizontal anisotropy.

Unified Fracture Design (UFD) Method

The UFD objective developed by Economides et al. (2002) for single phase Darcy PSS flow system, is to maximize the PSS productivity index for a fixed proppant volume. The following definition for the proppant number facilitates this objective:

$$N_p = 2\frac{k_f}{k}\frac{V_f}{V_r} \tag{1}$$

where k_f and V_f refer to the fracture permeability and volume, and k and V_r refer to reservoir permeability and drainage volume. The UFD method states that for a given proppant number, the PSS productivity Index, J_D, reaches its maximum value with a specific combination of fracture half-length and fracture width values. **Eq. 2** shows the definition of J_D in the UFD method:

$$J_D = \frac{B\mu}{2\pi kh}J \tag{2}$$

where J is the PSS productivity index given by the well rate, q, divided by the pressure difference, $\bar{p} - p_{wf}$.

In order to find the optimum J_D for the calculated value of N_p, the authors developed sensitivity studies showing J_D for a hydraulically fractured well in a square drainage area as a function of N_p and C_{fD}. **Figure 1 (Top)** shows that for values of $N_p < 0.1$ J_{Dmax} occurs for $C_{fD,opt} = 1.6$, where:

$$C_{fD} = \frac{k_f w}{k x_f} \tag{3}$$

For values of $N_p > 0.1$, Figure 1 **(Bottom)** shows a proportional relationship between the N_p and the optimum C_{fD} values for the given fracture volume. When the value of N_p is greater than 6, the optimum design is obtained when the fracture fully penetrates the well drainage area. Equations exist for calculating J_{Dmax} and $C_{fD,opt}$ for any proppant number. Once $C_{fD,opt}$ is known, the design fracture half-length and width are determined from the following equations.

$$x_f = \left(\frac{V_f k_f}{C_{fD,opt} h_f k}\right)^{1/2} \tag{4}$$

$$w = \left(\frac{C_{fD,opt} V_f k}{h k_f}\right)^{1/2} = \frac{V_f}{x_f h_f} \tag{5}$$

It is very important to use the correct and corresponding values of V_f and h_f in order to obtain correct results from the last two steps of the process. Design values for fracture half-length and width are used to determine the fracturing fluid injection rate and proppant concentration schedule that will achieve the productivity-optimized fracture design.

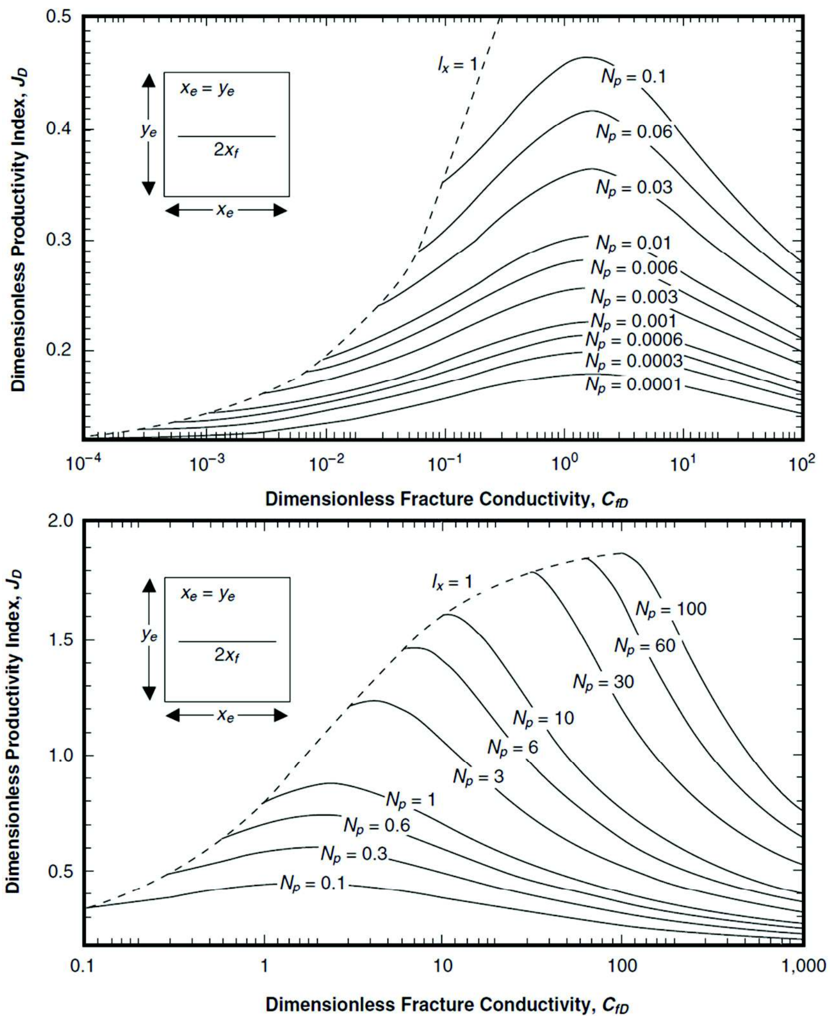

Figure 1: Dimensionless productivity index as a function of dimensionless fracture conductivity, with proppant number as a parameter. Top: for Np < 0.1. Bottom: for Np > 0.1 (Economides et al. 2002)

UFD Analog for a Horizontal Fracture

In an analogy to the vertical fracture, the proppant number for the horizontal fracture is given by

$$N_{p-HF} = \frac{k_f w r_f}{k_v r_e^2} = \frac{k_f}{k_v}\frac{V_f}{r_e^2}\frac{1}{\pi r_f}, \tag{6}$$

the horizontal fracture dimensionless conductivity is given by

$$C_{fD-HF} = \frac{k_f w}{k_v r_f}, \tag{7}$$

and the dimensionless productivity index is given by

$$J_D = \frac{B\mu}{2\pi k_v h} J \tag{8}$$

Numerical Model for the Horizontal Fracture in a Finite Circular Drainage Volume

A commercial reservoir numerical simulator was used to model the horizontal fracture using a radial grid with 50 cells in the R direction, 1 cell in the theta direction and 11 cells in the z direction. The horizontal fracture was modeled as the middle layer in the z direction; the rest of the cells in that direction had a fixed thickness of 2 ft giving a reservoir thickness of 20 ft. The well was located in the center of the model and had a radius of 0.3 ft. for all cases. It was only completed in the fracture, resulting in no flow directly from the reservoir to the wellbore. As such, all flow occurs from the reservoir to the fracture, and then from the fracture to the wellbore. **Figure 2** shows a diagram of the numerical model grid.

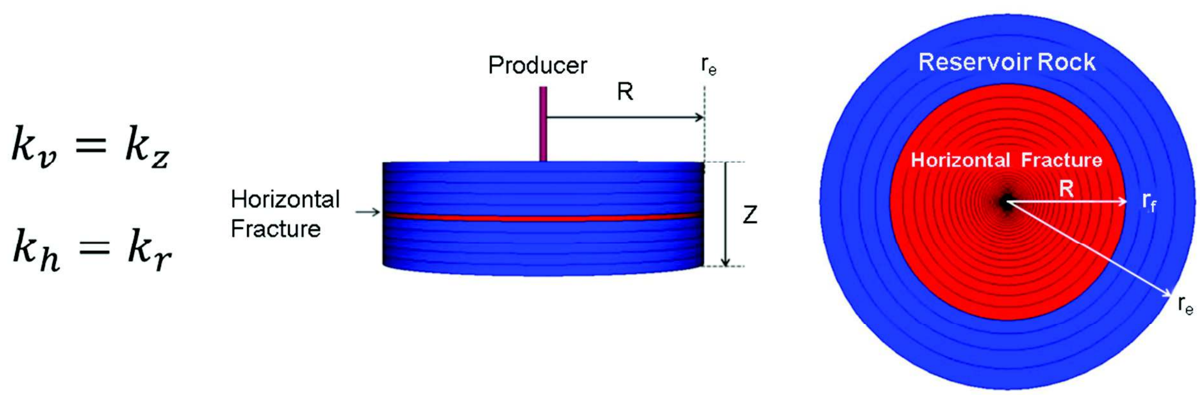

Figure 2: Grid configuration. Left: permeability orientation. Center: lateral view. Right: top view sliced at the level of the horizontal

Sensitivity studies considered values for the reservoir aspect ratio, $2r_e/h$, of 10, 20, and 50 and for vertical to horizontal permeability anisotropy, k_v/k_h, of 0.01, 0.1, and 1. The 2-dimensional numerical model did not support horizontal permeability anisotropy.

For each horizontal fracture model, model inputs started with selected values for the proppant number, fracture width, drainage radius, vertical and horizontal permeability, and fracture permeability. Then Eq. 6 provided a fracture radius consistent with the proppant number, and Eq. 7 provided the dimensionless fracture conductivity. All 63 cases presented in **Table 1** were computed.

Table 1: Simulation cases run for analysis of horizontal fracture performance

k_v/k_h	$2r_e/h$		
	10	20	50
0.01			
0.1	$N_{p\text{-}HF}$ = 0.0001, 0.001, 0.01, 0.1, 1, 10, 100		
1			

No skin was considered for the fracture, or the formation. Reservoir porosity was 0.1 and total compressibility of the system 13 x 10^{-6} psi^{-1}. The fluid in the reservoir was under saturated oil with a viscosity of 1 cp and a volumetric factor of 1 STB/RB.

The output from the simulations was used to calculate the productivity index for each case. To facilitate and generalize the use of the knowledge generated in this research, all the data presented has been displayed in dimensionless parameters.

Results and discussion

For horizontal fractures, because linear flow to the fracture is governed by vertical permeability, equations for proppant number and dimensionless fracture conductivity use vertical instead of horizontal permeability, and vertical to horizontal permeability anisotropy is expected to have a deep influence in well performance. Based on that, the following discussion is organized by permeability anisotropy.

Dimensionless horizontal fracture productivity index behavior as a function of dimensionless fracture conductivity and proppant number

For the isotropic reservoirs (k_v/k_h = 1), the behavior of the dimensionless productivity index as a function of dimensionless horizontal fracture conductivity for different aspect ratios and different proppant numbers is shown in **Figure 3 (Left).** Contrary to what have been established for vertical fractures, there is no convergence of the maximum dimensionless productivity index at any value of dimensionless fracture conductivity for any proppant number.

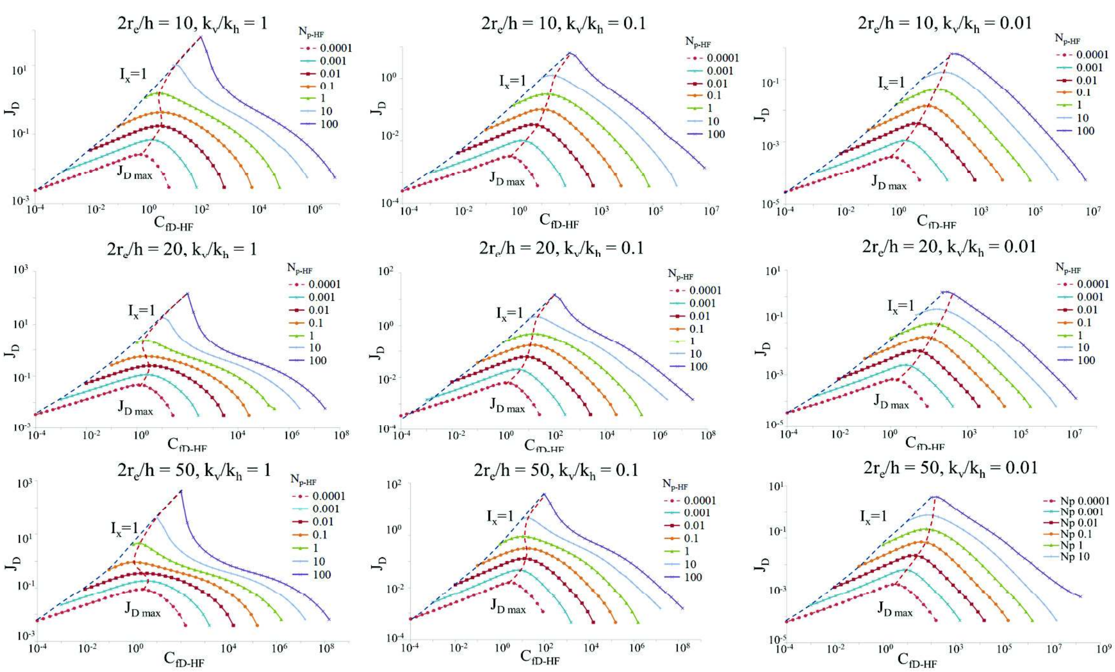

Figure 3: Dimensionless productivity index (J_D) as a function of dimensionless conductivity of the horizontal hydraulic fracture ($C_{fD\text{-}HF}$) for different proppant numbers (N_p) and different aspect ratios ($2r_e/h$). Left: isotropic reservoir. Center: anisotropic reservoir. Right: highly anisotropic reservoir.

Regardless of the aspect ratio, a horizontal fracture in an isotropic reservoir will have to be fully penetrating (I_x = 1) to achieve optimum well performance for proppant numbers equal or above 10 (N_{p-HF} >= 10); this statement could be also extrapolated to proppant numbers equal to unity (N_{p-HF} = 1) with a minor loss in productivity. However, for proppant numbers equal or below to 0.01 (N_{p-HF} <= 0.01) a fully penetrating fracture will not result in the best productivity for the well.

For anisotropic (k_v/k_h = 0.1) and highly anisotropic reservoirs (k_v/k_h = 0.01), Figure 3 **(Center and Right)** shows that a fully penetrating fracture (I_x = 1) can only be used for very high proppant numbers (N_{p-HF} >= 100), since it will not lead to the highest well performance for lower values of the proppant number. In those cases, the horizontal hydraulic fracture design has to be based on a determination of the optimal fracture conductivity for the desired proppant number using the relationships discussed in the next section**.** That approach is also encouraged because, as in the case of isotropic reservoirs, different proppant numbers exhibit different optimal fracture dimensionless conductivity values.

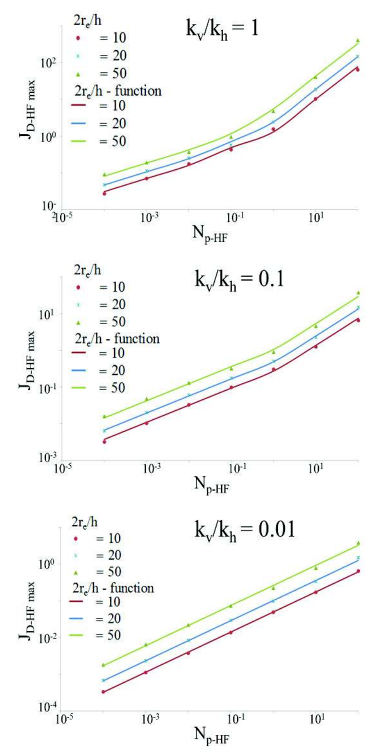

Figure 4: Dimensionless horizontal fracture maximum productivity index as a function of proppant number for different aspect ratios.

Maximum dimensionless horizontal fracture productivity index as a function of proppant number

The maximum dimensionless horizontal fractures productivity index ($J_{D\ max}$) as a function of proppant number (N_{p-HF}) is presented in **Figure 4**. In all cases; isotropic, anisotropic and highly anisotropic reservoirs, the horizontal fracture productivity index increases as proppant number and reservoir aspect ratio increases.

The maximum dimensionless productivity index can be estimated using the relationships in **Table 2** for a selected proppant number and a known reservoir aspect ratio. The good agreement of the functions and the simulation results is evidenced in Figure 4, where the lines correspond to the output of the functions in Table 2, and the points correspond to the output of the simulations. For isotropic reservoirs the behavior was fitted in three regions with three equations. The anisotropic case shows two regions yielding two equations, while the highly anisotropic reservoirs have just one trend that can be modeled with one equation.

Optimal horizontal fracture conductivity behavior as a function of proppant number

The optimal dimensionless conductivity for the horizontal fracture ($C_{fD-HF\ opt}$) is the dimensionless conductivity at which the maximum productivity index occurs ($J_{D\ max}$). For isotropic, anisotropic and highly anisotropic reservoirs, **Figure 5** shows optimal dimensionless horizontal fracture conductivity as a function of the proppant number for different aspect ratios. For proper horizontal fracture design, **Table 3** provides a set of equations to estimate optimal dimensionless horizontal fracture conductivity for a wide range of proppant numbers in a reservoir of known aspect ratio. The validity of the functions is supported by the good agreement shown in Figure 5 where the lines correspond to the output of the equations while the points are the results of the simulation work.

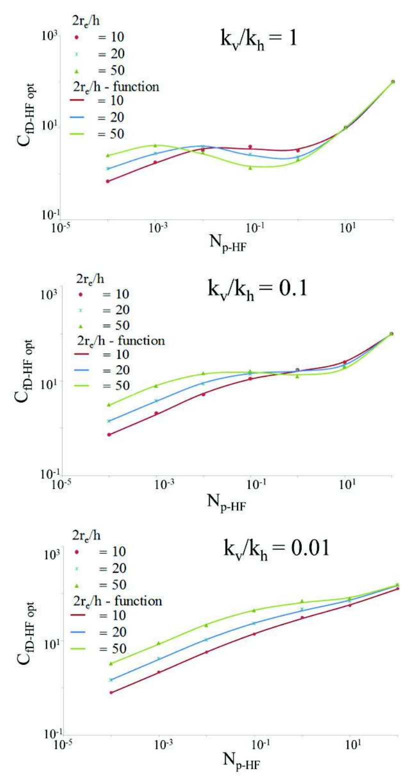

Figure 5: Dimensionless optimum horizontal fracture conductivity behavior as a function of proppant number for different aspect ratios.

Table 2: Maximum dimensionless horizontal fracture productivity index.

$k_v/k_h = 1$	$0.0001 \leq N_{p-HF} \leq 0.01$	$ln(J_{D,max}) = -1.56805 + 0.60138 ln\left(\frac{2r_e}{h}\right) + 0.35804 ln(N_{p-HF})$ $R^2 = 0.9881$
	$0.01 < N_{p-HF} < 1$	$ln(J_{D,max}) = -0.81286 + 0.54532 ln\left(\frac{2r_e}{h}\right) + 0.5078 ln(N_{p-HF})$ $R^2 = 0.9784$
	$1 \leq N_{p-HF} \leq 100$	$ln(J_{D,max}) = -1.8057 + 0.89694 ln\left(\frac{2r_e}{h}\right) + 0.88896 ln(N_{p-HF})$ $R^2 = 0.9953$
$k_v/k_h = 0.1$	$0.0001 \leq N_{p-HF} \leq 1$	$ln(J_{D,max}) = -3.22308 + 0.83824 ln\left(\frac{2r_e}{h}\right) + 0.46564 ln(N_{p-HF})$ $R^2 = 0.9968$
	$1 < N_{p-HF} \leq 100$	$ln(J_{D,max}) = -3.22948 + 0.84919 ln\left(\frac{2r_e}{h}\right) + 0.73495 ln(N_{p-HF})$ $R^2 = 0.9908$
$k_v/k_h = 0.01$	$0.0001 \leq N_{p-HF} \leq 100$	$ln(J_{D,max}) = -5.38051 + 1.03410 ln\left(\frac{2r_e}{h}\right) + 0.54643 ln(N_{p-HF})$ $R^2 = 0.9990$

Table 3: Optimum fracture conductivity, $C_{fD,opt}$ function

$k_v/k_h = 1$		$ln(C_{fD,opt}) = -5.1 \cdot 10^{-4} + 1.76 \cdot 10^{-4} ln\left(\frac{2r_e}{h}\right) + f\left(ln(N_{p-HF})\right), \quad R^2 = 0.9988$
	$2r_e/h=10$	$x = ln(N_{p-HF}),$ $f(x) = -1.2972 \cdot 10^{-4}x^5 - 1.0890 \cdot 10^{-3}x^4 + 1.2329 \cdot 10^{-2}x^3 + 0.10292x^2 + 0.16131x + 1.2398$
	$2r_e/h=20$	$x = ln(N_{p-HF}),$ $f(x) = -2.2254 \cdot 10^{-4}x^5 - 2.6554 \cdot 10^{-3}x^4 + 9.3069 \cdot 10^{-3}x^3 + 0.15737x^2 + 0.25273x + 0.85183$
	$2r_e/h=50$	$x = ln(N_{p-HF}),$ $f(x) = -1.1065 \cdot 10^{-4}x^5 - 2.0625 \cdot 10^{-3}x^4 + 8.5015 \cdot 10^{-4}x^3 + 0.14559x^2 + 0.42361x + 0.63608$
$k_v/k_h = 0.1$		$ln(C_{fD,opt}) = 0.05785 - 0.01581 ln\left(\frac{2r_e}{h}\right) + 0.99989 f\left(ln(N_{p-HF})\right), \quad R^2 = 0.9990$
	$2r_e/h=10$	$x = ln(N_{p-HF}),$ $f(x) = 5.7432 \cdot 10^{-4}x^4 + 8.1097 \cdot 10^{-3}x^3 + 4.9187 \cdot 10^{-3}x^2 + 0.14188x + 2.7858$
	$2r_e/h=20$	$x = ln(N_{p-HF}),$ $f(x) = 6.7621 \cdot 10^{-4}x^4 + 1.0546 \cdot 10^{-2}x^3 + 1.5117 \cdot 10^{-2}x^2 + 3.6515 \cdot 10^{-2}x + 2.7739$
	$2r_e/h=50$	$x = ln(N_{p-HF}),$ $f(x) = 5.2064 \cdot 10^{-4}x^4 + 1.0921 \cdot 10^{-2}x^3 + 3.7030 \cdot 10^{-2}x^2 - 1.7659 \cdot 10^{-2}x + 2.6140$
$k_v/k_h = 0.01$		$ln(C_{fD,opt}) = -1.7 \cdot 10^{-4} + 2.35 \cdot 10^{-5} ln\left(\frac{2r_e}{h}\right) + 1.000029 f\left(ln(N_{p-HF})\right), \quad R^2 = 0.9994$
	$2r_e/h=10$	$x = ln(N_{p-HF}),$ $f(x) = 1.6006 \cdot 10^{-4}x^4 + 1.7647 \cdot 10^{-3}x^3 - 7.9051 \cdot 10^{-3}x^2 + 0.29686x + 3.3921$
	$2r_e/h=20$	$x = ln(N_{p-HF}),$ $f(x) = 2.1007 \cdot 10^{-4}x^4 + 2.6546 \cdot 10^{-3}x^3 - 8.1725 \cdot 10^{-3}x^2 + 0.22978x + 3.7675$
	$2r_e/h=50$	$x = ln(N_{p-HF}),$ $f(x) = 3.7882 \cdot 10^{-4}x^4 + 4.6142 \cdot 10^{-3}x^3 - 1.2630 \cdot 10^{-2}x^2 + 0.11076x + 4.1645$

For isotropic reservoirs, when proppant number is low (N_{p-HF} < *0.002*), higher reservoir aspect ratios will require higher fracture conductivity to achieve maximum productivity, compared to reservoirs with lower aspect ratios. The plot then shows a transition zone after which the trend is reversed for proppant number above 0.02 (N_{p-HF} > *0.02*). For larger proppant numbers (N_{p-HF} > *10*), optimal fracture conductivity is independent on the reservoir aspect ratio and is only a function of proppant number.

In anisotropic reservoirs, when proppant number is below 0.01, higher reservoir aspect ratios will require higher fracture conductivity to achieve maximum productivity. A transition zone is observed for proppant numbers between 0.1 and 1 after which the trend is reversed; however, for the range of the plot where lower reservoir aspect ratios have higher optimal fracture conductivity, aspect ratio influences the behavior to a lesser degree. The convergence of the lines at the end of the plot is an indication that for proppant numbers above 100, reservoir aspect ratio no longer influences the behavior of optimal fracture conductivity.

For the highly anisotropic reservoirs, generally speaking, the optimum fracture conductivity will be higher as the reservoir aspect ratio is higher. The degree of influence of reservoir aspect ratio over optimum fracture conductivity is reduced as the proppant number increases. For proppant numbers above 10 such influence is already small.

Example Application

For k_v/k_h = 1, k_h = 1md, h = 30 ft, r_e = 750 ft, proppant mass 100,000 lb, proppant density 2.65 g/cc, proppant porosity 0.4, and proppant permeability k_f = 60,000 md, determine the fracture radius and width that maximizes the well productivity.

For this example $2r_e/h$ = 50. From the proppant mass, the volume of the fracture is V_f = 100,000/[(2.65)(62.4)(1-0.4)] = 1008 ft^3. The calculation requires iteration on r_f. Assuming an initial value for r_f = 100 ft, the proppant number calculated from Eq. 6 is

$$N_{p-HF} = \frac{60{,}000}{1}\frac{1008}{750^2}\frac{1}{3.14(100)} = 0.342 \quad (9)$$

From the appropriate equation in Table 3, the optimal dimensionless fracture conductivity ($C_{fD-HF\ \mathrm{opt}}$) for the isotropic case is 1.4. From the calculated fracture volume and for the assumed r_f, w = 1008/[π(100)^2] = 0.385 in. From Eq. 7, the dimensionless fracture conductivity is

$$C_{fD-HF} = \frac{(60{,}000)(0.0321)}{(1)(100)} = 19.2 \quad (10)$$

Adjusting to reach convergence results in the optimized fracture design with r_f = 240 ft, w = 0.067 in, N_{p-HF} = 0.143, C_{fD-HF} = 1.4, and J_{Dmax} = 1.4 using the appropriate equation in Table 2.

It might be noted that the resultant optimal propped fracture width is barely larger than 3 times the diameter of typical 20/40 mesh sand proppant. Further iterations are now easy to apply should an operator wish to investigate width constraints with respect to various mesh size proppants and fracture conductivities, while directly observing what the predicted impact on fracture productivity should be.

Conclusions

This work has related dimensionless parameters for proppant number, reservoir aspect ratio and reservoir anisotropy to optimal dimensionless horizontal fracture conductivity values that can be used to determine fracture design parameters that maximize horizontal fracture dimensionless productivity index.

Unlike for vertical fractures, for horizontal fractures, there is no convergence of maximum dimensionless productivity index for different proppant numbers at any value of dimensionless fracture conductivity.

For isotropic reservoirs, a fully penetrating facture will yield maximum productivity when proppant number is above 10 regardless of the reservoir aspect ratio. For proppant numbers below 10, fracture design based on the optimal dimensionless fracture conductivity is encouraged.

In anisotropic reservoirs, the maximum productivity for the hydraulic horizontal fracture can be achieved with a fully penetrating fracture when the proppant number is above 100 regardless of reservoir aspect ratio. In all other cases, the design based in the determination of optimal dimensionless fracture conductivity is required.

In highly anisotropic reservoirs, it is always recommended to design based on the determination of the optimal dimensionless fracture conductivity.

Mathematical expressions have been provided, which can be used to accurately determine optimum fracture dimensionless conductivity and the maximum productivity index based on proppant number, anisotropy and reservoir aspect ratio. These expressions can be programed on spreadsheets or any commercial programming language to automate the proposed fracture design workflow.

Nomenclature

B = formation volume factor, RB/STB
C_{fD} = dimensionless fracture conductivity
C_{fD-HF} = dimensionless fracture conductivity for horizontal fracture
h = formation thickness, ft
h_f = fracture height, ft
I_x = fracture penetration ratio, x_f/x_e, dimensionless
J = productivity index, STB/psi
J_D = dimensionless productivity index
k = matrix (formation) permeability, md
k_f = fracture permeability, md
k_h = horizontal formation permeability, md
k_v = vertical formation permeability, md
k_x = x-direction formation permeability, md
k_y = y-direction formation permeability, md
k_z = z-direction formation permeability, md
N_p = proppant number, dimensionless
N_{p-HF} = proppant number for horizontal fracture, dimensionless
r_e = reservoir (drainage) equivalent radius, ft
r_f' = fracture equivalent radius, ft
r_w = wellbore radius, ft
s_f = pseudo fracture skin factor
x_e = half length of the drainage area, ft
x_f = half length of the fracture, ft
y_e = width (y-direction) of the drainage area, ft
V_f = one propped wing (fracture) volume, ft^3
w = average propped fracture width, ft

Greek variables

μ = viscosity, cp

SI Metric Conversion Factors

bbl	x 1.589873E-1	= m^3
ft	x 3.048E-1	= m
°C	x 9/5+32	= °F
cp	x 1E-3	= Pa.s
psia	x 6894.76	= Pa

Acknowledgments

The work presented in this paper was the result of a project developed as part of the Pressure Transient Test (PETE 648) course at the Harold Vance Department of Petroleum Engineering of Texas A&M University, during summer 2012. Simulation work was a joint effort performed by all the students. Moreover, the discussion inside the classroom played an important role overcoming the difficulties found during the development of this research. Therefore, the authors are pleased to acknowledge all graduate students in the class, especially Peerapong Ekkawong, for their valuable contribution. The authors also wish to thank Schlumberger for use of the Eclipse simulator.

References

Cinco-Ley, H. and Samaniego-V., F. 1981. Transient Pressure Analysis for Fractured Wells. *Journal of Petroleum Technology* **33** (9): 1749-1766. DOI: 10.2118/7490-pa

Daal, J.A. and Economides, M.J. 2006. Optimization of Hydraulically Fractured Wells in Irregularly Shaped Drainage Areas. Paper presented at the International Symposium and Exhibition on Formation Damage Control, Lafayette, Louisiana U.S.A. Society of Petroleum Engineers SPE-98047-MS. DOI: 10.2118/98047-ms.

Economides, M.J., Oligney, R., and Valkó, P.P. 2002. *Unified Fracture Design*. Alvin, Texas, USA.: Orsa Press. Original edition. ISBN.

Jamiolahmady, M., Sohrabi, M., and Mahdiyar, H. 2009. Optimization of Hydraulic Fracture Geometry. Paper presented at the Offshore Europe, Aberdeen, UK. Society of Petroleum Engineers SPE-123466-MS. DOI: 10.2118/123466-ms.

Larsen, L. 2011. Horizontal Fractures in Single and Multilayer Reservoirs. Paper presented at the Canadian Unconventional Resources Conference, Alberta, Canada. Society of Petroleum Engineers SPE-147004-MS. DOI: 10.2118/147004-ms.

Lopez-Hernandez, H.D., Valkó, P.P., and Pham, T.T. 2004. Optimum Fracture Treatment Design Minimizes the Impact of Non-Darcy Flow Effects. Paper presented at the SPE Annual Technical Conference and Exhibition, Houston, Texas. Society of Petroleum Engineers 00090195. DOI: 10.2118/90195-ms.

Valkó, P.P. and Economides, M.J. 1998. Heavy Crude Production from Shallow Formations: Long Horizontal Wells Versus Horizontal Fractures. Paper presented at the SPE International Conference on Horizontal Well Technology, Calgary, Alberta, Canada. Copyright 1998, Society of Petroleum Engineers Inc. 00050421. DOI: 10.2118/50421-ms.